

Moderate hydrogen bond network via in-situ dissolved interfacial cationic solvation effect for highly active aqueous zinc-manganese batteries

Mengting Cheng^a, Wei Yin^a, Yuzhu Wang^a, Yijiao Geng^a, Yongzhong Wu^a, Jie Luo^a, Zhexuan Liu^{a,*}, Yongfeng Luo^{a,*}, Guozhao Fang^{b,*}

^a *State Key Laboratory of Utilization of Woody Oil Resources, Hunan Province Key Laboratory of Materials Surface & Interface Science and Technology, School of Chemistry and Chemical Engineering, School of Materials and Energy, Central South University of Forestry and Technology, Changsha, Hunan 410004, P.R. China*

^b *School of Materials Science and Engineering, Key Laboratory of Electronic Packaging and Advanced Functional Materials of Hunan Province, Central South University, Changsha, Hunan 410083, P.R. China*

*Corresponding author.

E-mail address: lzxuan@csuft.edu.cn (Z. Liu); yfluo@csuft.edu.cn (Y. Luo); fg_zhao@csu.edu.cn (G. Fang)

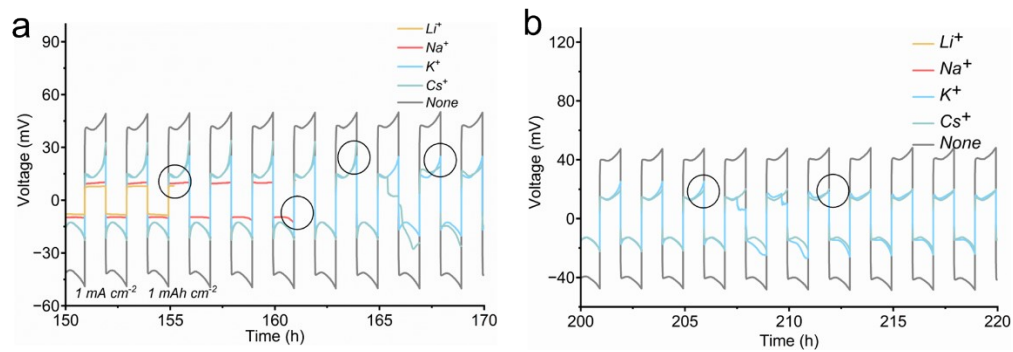


Figure S1. Suppressed cycle stability by alkali metal ion additives at current density of (a) 150 h-170 h and (b) 200 h-220 h.

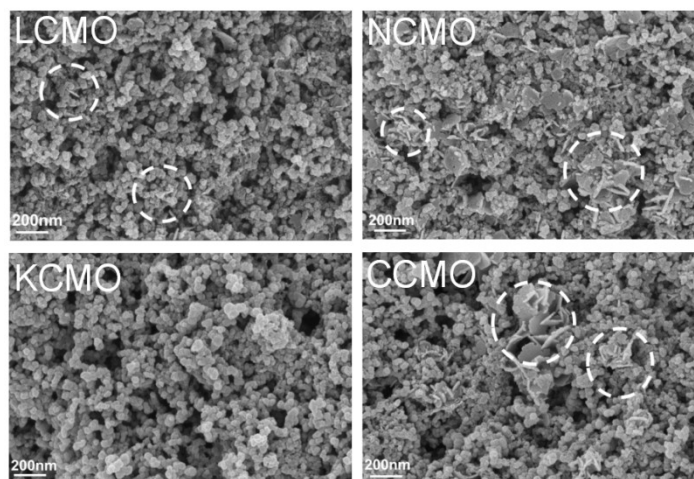


Figure S2. SEM images of LCMO, NCMO, KCMO, CCMO.

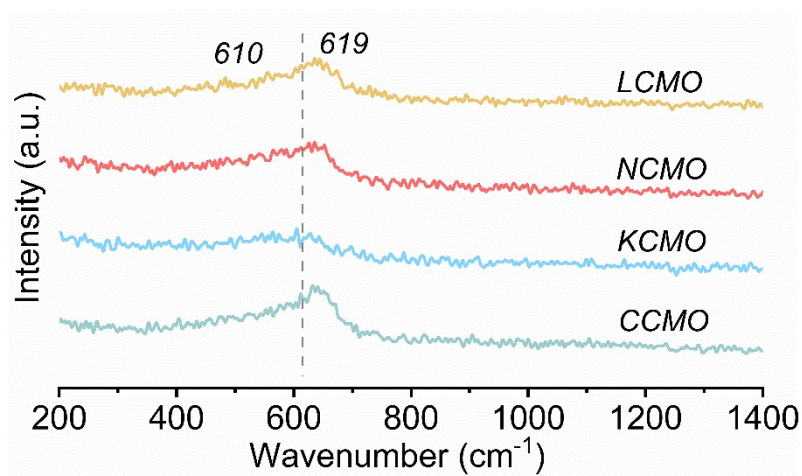


Figure S3. Powder Raman Spectra of LCMO, NCMO, KCMO and CCMO.

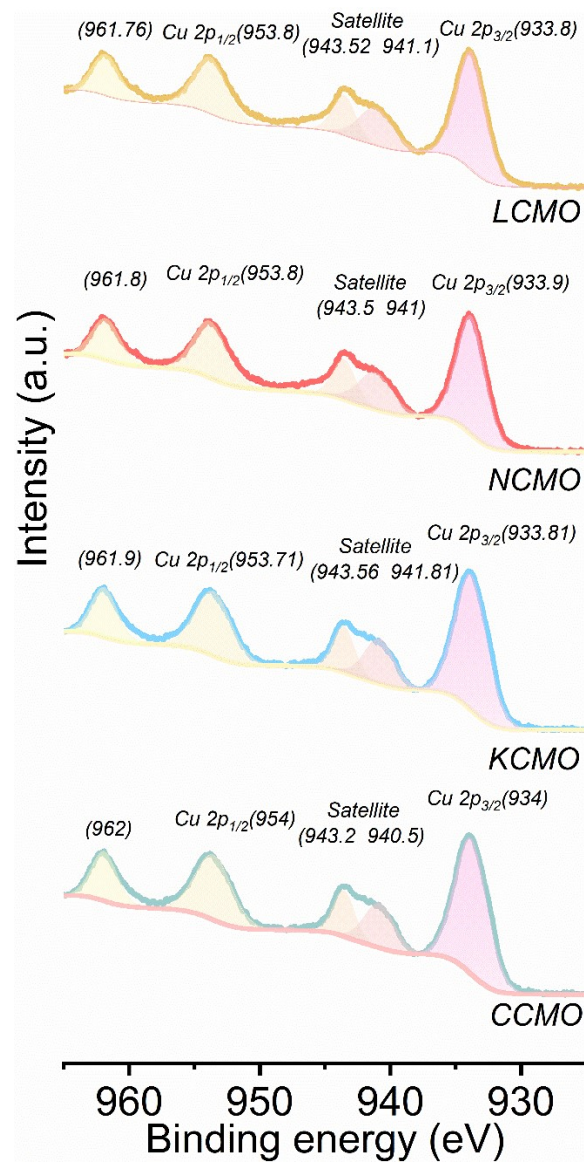


Figure S4. XPS Cu 2p spectra of LCMO, NCMO, KCMO, CCMO.

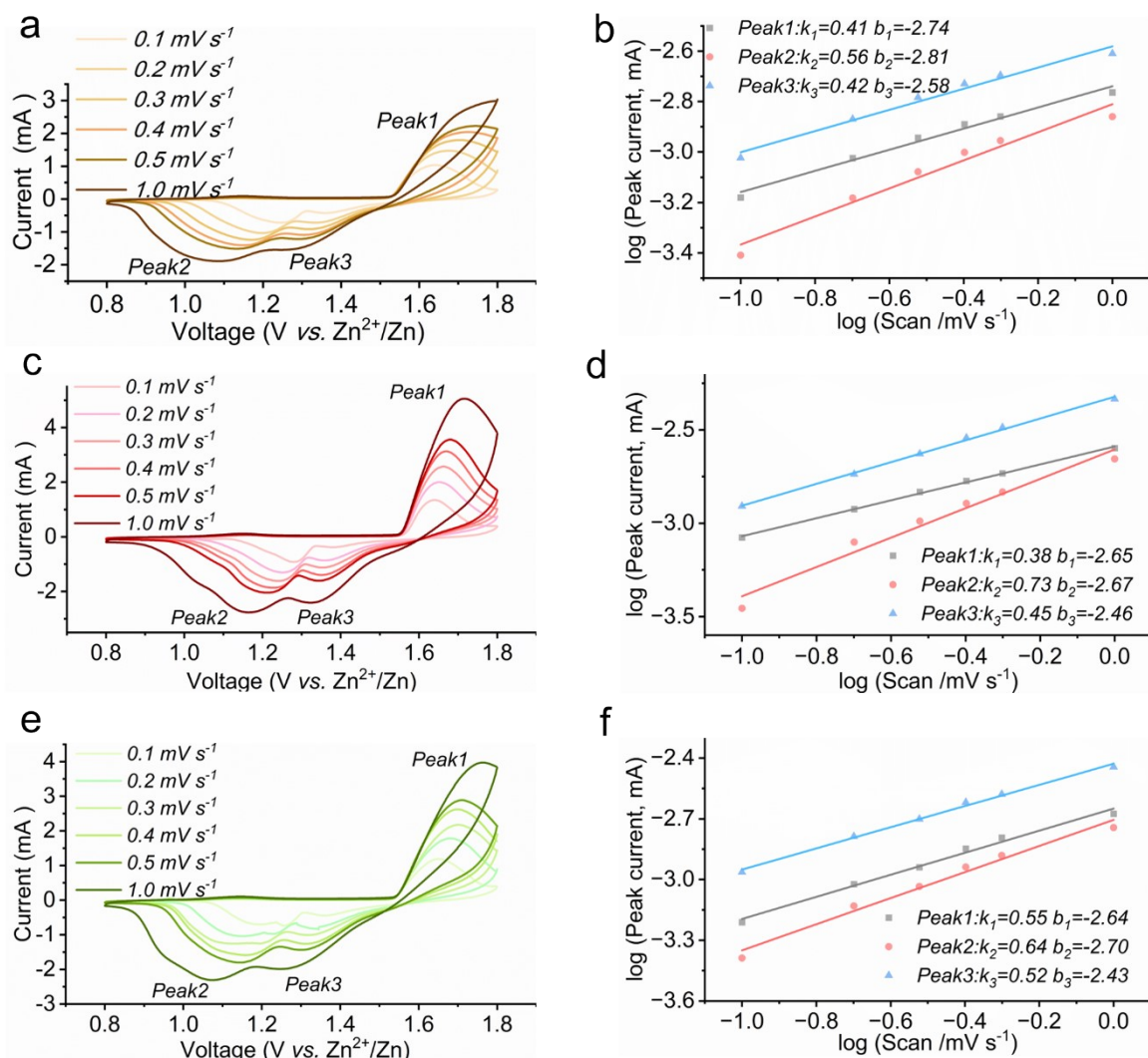


Figure S5 CV, k and b curves of (a), (b) LCMO, (c), (d) NCMO, (e), (f) CCMO at scan rates ranging from 0.1 mV s^{-1} to 1 mV s^{-1} .

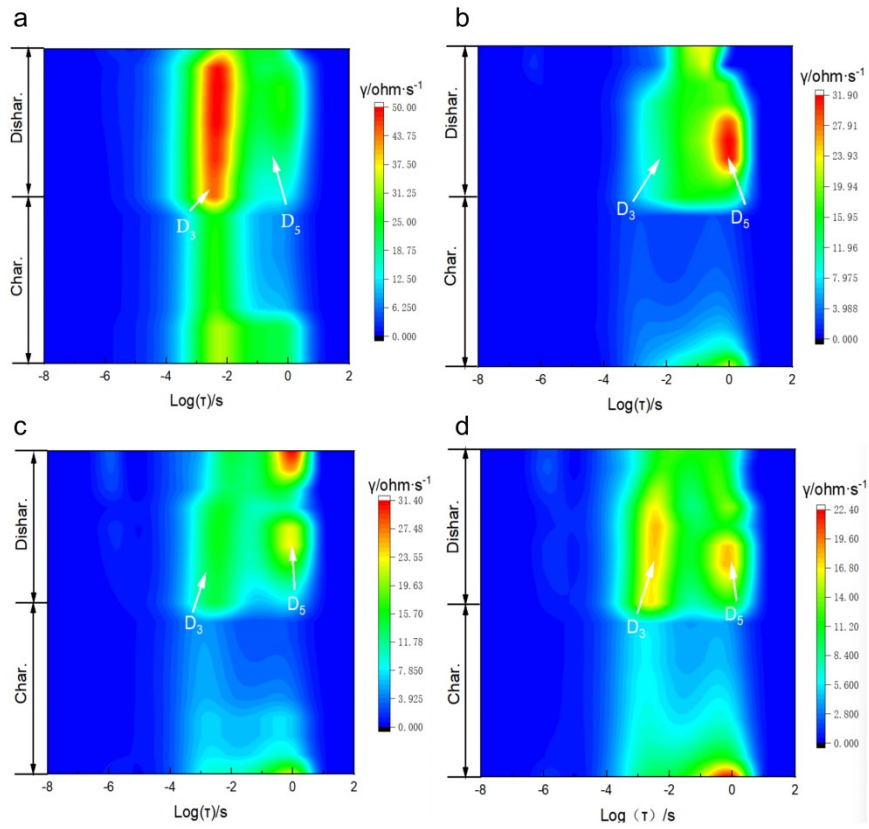


Figure S6. DRT spectra at the range of $10^{-8}\sim 10^2\text{s}$ in (a) LCMO (b) NCMO (c) KCMO (d) CCMO.